

University of Wollongong

Research Online

Australian Institute for Innovative Materials -
Papers

Australian Institute for Innovative Materials

1-1-2015

Terahertz probes of magnetic field induced spin reorientation in YFeO₃ single crystal

Xian Lin
Shanghai University

Junjie Jiang
Shanghai University

Zuanming Jin
Shanghai University

Dongyang Wang
Tianjin University

Zhen Tian
Tianjin University

See next page for additional authors

Follow this and additional works at: <https://ro.uow.edu.au/aiimpapers>



Part of the [Engineering Commons](#), and the [Physical Sciences and Mathematics Commons](#)

Research Online is the open access institutional repository for the University of Wollongong. For further information contact the UOW Library: research-pubs@uow.edu.au

Terahertz probes of magnetic field induced spin reorientation in YFeO₃ single crystal

Abstract

Using the terahertz time-domain spectroscopy, we demonstrate the spin reorientation of a canted antiferromagnetic YFeO₃ single crystal, by evaluating the temperature and magnetic field dependence of resonant frequency and amplitude for the quasi-ferromagnetic (FM) and quasi-antiferromagnetic modes (AFM), a deeper insight into the dynamics of spin reorientation in rare-earth orthoferrites is established. Due to the absence of 4f-electrons in Y ion, the spin reorientation of Fe sublattices can only be induced by the applied magnetic field, rather than temperature. In agreement with the theoretical predication, the frequency of FM mode decreases with magnetic field. In addition, an obvious step of spin reorientation phase transition occurs with a relatively large applied magnetic field of 4 T. By comparison with the family members of RFeO₃ (R = Y³⁺ or rare-earth ions), our results suggest that the chosen of R would tailor the dynamical rotation properties of Fe ions, leading to the designable spin switching in the orthoferrite antiferromagnetic systems.

Keywords

spin, reorientation, yfeo, 3, single, probes, crystal, magnetic, terahertz, field, induced

Disciplines

Engineering | Physical Sciences and Mathematics

Publication Details

Lin, X., Jiang, J., Jin, Z., Wang, D., Tian, Z., Han, J., Cheng, Z. & Ma, G. (2015). Terahertz probes of magnetic field induced spin reorientation in YFeO₃ single crystal. *Applied Physics Letters*, 106 (9), 092403-1-092403-4.

Authors

Xian Lin, Junjie Jiang, Zuanming Jin, Dongyang Wang, Zhen Tian, Jianguang Han, Zhenxiang Cheng, and Guohong Ma

Terahertz probes of magnetic field induced spin reorientation in YFeO₃ single crystal

Xian Lin,¹ Junjie Jiang,¹ Zuanming Jin,^{1,2} Dongyang Wang,³ Zhen Tian,³ Jianguang Han,³ Zhenxiang Cheng,^{1,4} and Guohong Ma^{1,a)}

¹Department of Physics, Shanghai University, Shanghai 200444, People's Republic of China

²Max Planck Institute for Polymer Research, Ackermannweg 10, 55128 Mainz, Germany

³Center for Terahertz Waves and College of Precision Instrument and Optoelectronics Engineering, Key Laboratory of Optoelectronics Information and Technology (Ministry of Education), Tianjin University, Tianjin 300072, People's Republic of China

⁴Institute for Superconducting and Electronic Materials, University of Wollongong, Wollongong, New South Wales 2522, Australia

(Received 16 January 2015; accepted 19 February 2015; published online 3 March 2015)

Using the terahertz time-domain spectroscopy, we demonstrate the spin reorientation of a canted antiferromagnetic YFeO₃ single crystal, by evaluating the temperature and magnetic field dependence of resonant frequency and amplitude for the quasi-ferromagnetic (FM) and quasi-antiferromagnetic modes (AFM), a deeper insight into the dynamics of spin reorientation in rare-earth orthoferrites is established. Due to the absence of *4f*-electrons in Y ion, the spin reorientation of Fe sublattices can only be induced by the applied magnetic field, rather than temperature. In agreement with the theoretical predication, the frequency of FM mode decreases with magnetic field. In addition, an obvious step of spin reorientation phase transition occurs with a relatively large applied magnetic field of 4 T. By comparison with the family members of RFeO₃ (R = Y³⁺ or rare-earth ions), our results suggest that the chosen of R would tailor the dynamical rotation properties of Fe ions, leading to the designable spin switching in the orthoferrite antiferromagnetic systems. © 2015 AIP Publishing LLC. [<http://dx.doi.org/10.1063/1.4913998>]

Motivated by the potential applications in spintronics and energy efficient information technology, external field induced spin reorientation transition (SRT) in rare-earth orthoferrites (RFeO₃, R = rare-earth ions or Y) attracts lots of interests;^{1–5} for example, the designable spin switching and magnetic recording. A key topic is to understand how does the R ion work during the SRT process, not only required by the fundamental physics involving Dzyaloshinskii-Moriya (DM) as well as R and Fe ions interactions but also required by the appealing designable spin switching in the antiferromagnetic systems. So far, several experimental techniques such as neutron diffraction,⁶ AC magnetic susceptibility measurements,⁷ nuclear magnetic resonance (NMR),⁸ ultrasound,⁹ and Mössbauer spectra¹⁰ were employed to study the SRT; yet, the probes of spin resonant excitation, coherent control, and dynamical switching of spins are heavily needed on sub-picosecond timescale.^{11–14}

Recently, the magnetic component of terahertz (THz) pulse has been employed to non-thermally excite and manipulate the spin precession through magnetic dipole coupling in RFeO₃.^{15,16} The temperature induced SRT in ErFeO₃ and NdFeO₃ has been investigated by employing THz-time domain spectroscopy (TDS) recently.^{17,18} Compared with the spin dynamics triggered by femtosecond laser pulse with inverse Faraday effect^{19,20} in which the electron transition and the heat caused by the high photon energy of the pulse is a hindrance to its future application, THz pulse is direct

impulsive excitation of spin precession motion by the magnetic component of the terahertz pulse, is free from electronic excitations because of its much lower photon energy, in the meantime avoiding the thermal effect that could disturbs the spin system. Also, using terahertz time domain spectroscopy, more information can be extracted such as the amplitude, lifetime, and phase of spin systems via ultrafast time-domain analysis, which cannot be obtained from the static experiments.

As an antiferromagnetic RFeO₃ crystal is illuminated by a THz pulse, the magnetic field component of the THz wave couples with the magnetic moment of the sample through a transient Zeeman torque $\mathbf{T} = \gamma \mathbf{M} \times \mathbf{H}_{\text{THz}}$, where γ denotes the gyromagnetic constant, \mathbf{M} and \mathbf{H}_{THz} are the macroscopic magnetization and the impulsive magnetic field of THz wave, respectively. Tipped out of the easy direction by \mathbf{T} , the tilting magnetic moment \mathbf{M} starts to precess around the effective magnetic field, which persists within the spin relaxation time. Two optically active spin resonance modes, quasi-ferromagnetic mode (FM) and quasi-antiferromagnetic mode (AFM), can be selectively excited as the \mathbf{H}_{THz} aligns perpendicular and parallel to the \mathbf{M} , respectively. The induced precession of the macroscopic magnetization is expected to radiate free induction decay (FID) signal with the magnetic resonance frequency. The frequencies and amplitudes of both two modes are sensitive to the geometry between \mathbf{H}_{THz} and \mathbf{M} . The amplitude of the FID signal is proportional to \mathbf{T} , which has the largest value when \mathbf{H}_{THz} is perpendicular to \mathbf{M} . Importantly, one can therefore expect the magnitude change of \mathbf{T} when SRT occurs (i.e., \mathbf{M} deviates the orientation of perpendicular to \mathbf{H}_{THz}). By recording

^{a)}Author to whom correspondence should be addressed. Electronic mail: ghma@staff.shu.edu.cn

the dependences of the spin resonance (such as amplitude and frequency) on temperature and magnetic field, detailed information about SRT can be obtained using THz-TDS.

As described by Dzyaloshinsky and Moriya, the low symmetry combined with spin-orbit coupling gives rise to anti-symmetric exchange interactions of RFeO_3 .^{21,22} Below Néel temperature and absent of external magnetic field, the magnetic structure corresponds to the irreducible representation Γ_4 phase (G_x, F_z) of iron orders with a weak ferromagnetic moment \mathbf{F} along c -axis ($c||z$, the x, y, z coordinate axes are set along a, b , and c axes of the crystal, respectively). The magnetic moment along one of the symmetry axis of the crystal is known as a symmetric phase.^{23,24} The temperature-induced spontaneous SRT in orthoferrites shows a sequence of transition $\Gamma_4 \rightarrow \Gamma_{24} \rightarrow \Gamma_2$ ($G_x F_z \rightarrow G_x F_z G_z F_x \rightarrow G_z F_x$, where \mathbf{F} and \mathbf{G} are the ferro- and antiferro-magnetism vectors, respectively). The sample system is transferred into another symmetric configuration Γ_2 ($\mathbf{F}||a$ -axis).^{17,18,24} Two second-order phase transition points defines a temperature range of SRT. Temperature-induced spin switching is mainly caused by the competition between Fe ions ($3d$ electron subsystem) and paramagnetic R ions ($4f$ electron subsystem). On the other hand, the weak ferromagnetic moment \mathbf{F} is expected to rotate from c -axis toward the direction of \mathbf{H}_{ext} as an external magnetic field (\mathbf{H}_{ext}) is applied along vector \mathbf{G} ($\mathbf{H}_{\text{ext}}||a$ -axis), which yields a progressive increase of the magnetization along a -axis.^{25,26}

As a family member of canted antiferromagnetic RFeO_3 , yttrium orthoferrites (YFeO_3) has no f electron in Y^{3+} ions. Owing to the nonmagnetic characteristic of Y ions, YFeO_3 is an excellent candidate for investigation of external magnetic field induced SRT of iron sublattice, avoiding the complex exchange interaction between rare-earth ions and Fe ions under magnetic field, in particular. A single crystal of YFeO_3 was grown by the optical floating-zone method. The sample (c -cut, 1.33 mm thick) is polished on both sides for THz measurements. The all fiber-based THz-TDS integrated with the strong-magnetic field and a low-temperature system was used for TDS measurement. The emitter of the THz-TDS was excited by a 1560 nm laser pulse. The sample was mounted in the Oxford Instruments Spectromag He-bath cryostat (SHC) placed in a collimated terahertz beam. The THz pulse that transmitted through the sample was focused onto the receiver. The temperature ranges from 1.5 to 260 K and the magnetic field is up to the maximum value of 7 T. The temperature- and magnetic field-fluctuation of the SHC was well controlled within 0.01 K and 1 mT, respectively. The spectral range of the THz we used from 0.1 to 1.5 THz, centered at 0.6 THz and the signal to noise ratio was 1000:1. The THz pulse scans were measured with a time range of 30 ps, corresponding to a spectral resolution of about 0.03 THz.

Typical THz-TDS in time-domain and its Fourier transform spectrum of YFeO_3 have been represented in our previous papers and supplementary material.^{16,27,28} A zoomed-in section of the transmittance of THz waveform is shown in the inset of Fig. 1, a resonant dip at around 0.29 THz corresponds to the FM mode at room temperature. Figure 1 presents the resonant frequency and amplitude of the FM spin-wave mode as a function of temperature. The resonant

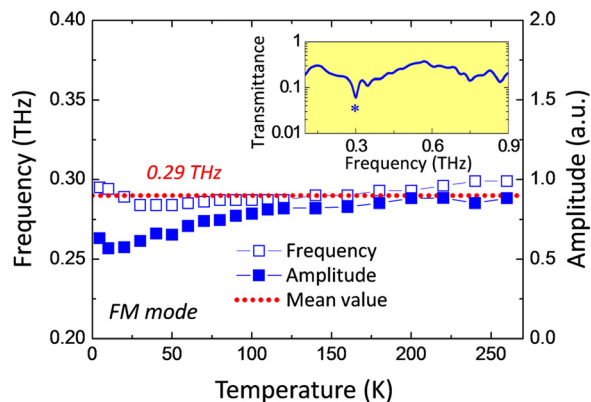


FIG. 1. The resonance frequency and the spectral amplitude of FM mode in the c -cut YFeO_3 single crystal are shown as functions of temperature. The frequency is obtained from the dip in transmittance spectra (inset), which is calculated by the ratio of the Fourier transformed spectrum to a reference spectrum at room temperature.

frequency of FM mode shows mostly temperature independence with a mean value of 0.29 THz, as shown by the dashed line in Fig. 1. Additionally, the amplitude of FM mode decreases slightly as the sample is cooled. We do not observe any other resonances at higher frequency range, which means that AFM mode in YFeO_3 has never been available for the c -cut sample in the whole temperature range. In contrast to the temperature-induced SRT in NdFeO_3 , the SRT of Fe^{3+} sublattice is ascribed to the exchange interaction between $\text{Nd-}4f$ and $\text{Fe-}3d$ electrons, either theoretically or experimentally.¹⁸ Indeed, SRT in YFeO_3 cannot be triggered by temperature, due to the absence of $4f$ electron in Y ion, which makes YFeO_3 be different from other common rare-earth orthoferrites, such as ErFeO_3 , NdFeO_3 , and TmFeO_3 , etc., in which the ferromagnetic vector \mathbf{F} rotates by 90° as the temperature is varied across characteristic SR temperatures, YFeO_3 stays in the Γ_4 phase from T_N to the temperature as low as a few Kelvin. Our THz-TDS data is consistent with previous measurements.²⁹

In the following, we focus on the study of magnetic field induced SRT in YFeO_3 . The magnetic field of THz pulse and external magnetic field are set parallel to the a -axis of YFeO_3 crystal ($\mathbf{H}_{\text{ext}}||\mathbf{H}_{\text{THz}}||a$ -axis). The time resolved signals are first converted into the frequency domain by Fourier transformation. The normalized loss function, $\alpha(\omega)$, including both reflective and absorptive losses, is given by Beer–Lambert law

$$\alpha(\omega) = -\ln\left(\left|\frac{T(\omega)}{T_{\text{ref}}(\omega)}\right|\right), \quad (1)$$

where $T(\omega)$ is the transmitted spectrum of the THz signal at different values of external magnetic field and $T_{\text{ref}}(\omega)$ is the reference spectrum transmitted through the system without sample at zero magnetic field. According to Eq. (1), Figs. 2(a) and 2(b) show the amplitude mapping of the THz loss spectrum in two frequencies ranges from 0.48 to 0.6 THz and 0.2 to 0.36 THz, respectively, at 260 K. As shown in Fig. 2(b), the resonant absorption peak corresponding to the FM mode, which exhibits continuous softening from 0.29 to 0.21 THz, as the external magnetic field is increased from 0 to 7 T.

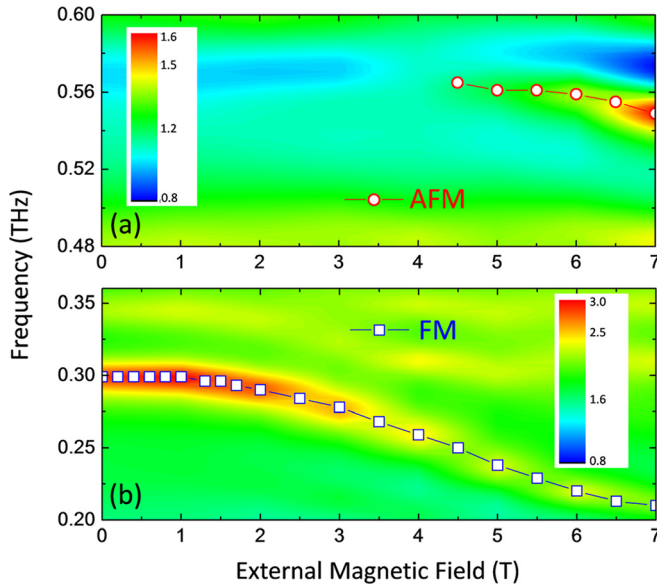


FIG. 2. The amplitude mapping of the loss function, as a function of the external magnetic field along a -axis, in the cases of two spectrum regions: AFM mode (a) and FM mode region (b) at temperature of 260 K.

At lower applied magnetic field ($H < 2$ T), the frequency of FM mode keeps relative constant, which indicates that the phase of YFeO_3 crystal changes slowly when the applied magnetic field is below 2 T. We can hardly see any absorption peak in the high frequency range with lower magnetic field, as shown in Fig. 2(a). By increasing the magnitude of H above 2 T, the frequency of FM-mode starts to decrease quickly with magnetic field, and the mode is still observable with the field up to 7 T. The frequency softening of FM-mode is indicative of the appearance of SRT induced by magnetic field. On the other hand, the FM-mode persists up to 7 T implies the SRT does not complete under the field of 7 T. It is important to note that a higher resonant frequency at 0.55 THz is clearly observed at the magnetic field of 4 T, and this frequency mode decreases slightly with the magnetic field, as shown in Fig. 2(a). According to our experimental results, we can conclude that the YFeO_3 is Γ_4 phase without magnetic field, and the crystal is transformed into Γ_{24} phase when apply the magnetic field. Previous studies revealed that the SRT is completed under a critic magnetic field $H_{cr} = 7.4$ T.³⁰ As the highest magnetic field is 7 T in our system, the Γ_2 phase of YFeO_3 cannot be reached in the present condition.

In a qualitative picture, as the magnetic-field of incident THz pulse is perpendicular to the vector \mathbf{F} of YFeO_3 , the observed oscillation at a frequency of 0.29 THz is due to the FM spin resonance mode. Under external magnetic field, as shown in the inset of Fig. 3(a), the magnetic moment rotates from the c -axis to a -axis in ac -plane, corresponding to the SRT from Γ_4 to Γ_2 via Γ_{24} . Our experimental observation of the oscillation at 0.55 THz, therefore, can be explained by the excitation of AFM spin resonance mode, as the vector \mathbf{F} has the component along the magnetic-field of THz pulse.

This reorientation behavior can also be observed in Fig. 3(a), which shows the magnetic-field dependent spectral amplitudes of FM and AFM modes. The spectral amplitude here is extracted by the full width at half maximum

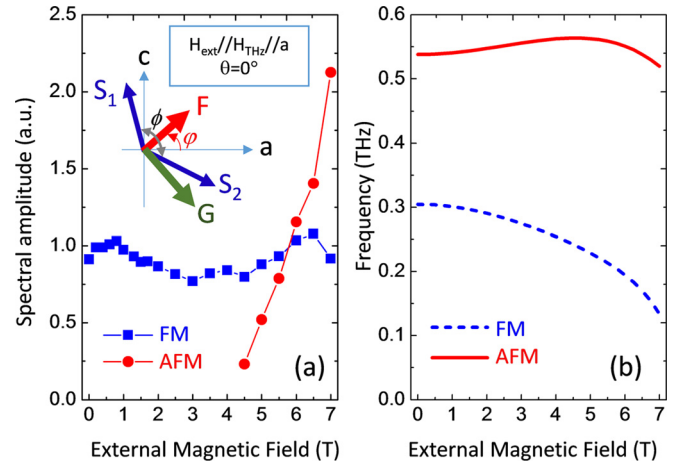


FIG. 3. (a) Spectral amplitudes of FM mode (blue squares) and AFM mode (red dots) are shown as functions of applied magnetic field. Inset shows the sketch of the simplified magnetic configuration in YFeO_3 upon the spin reorientation process. \mathbf{S}_1 and \mathbf{S}_2 are two pairs of spins for Fe^{3+} sublattices. (b) Results of the calculation of the frequencies of the FM and AFM modes as functions of external magnetic field, where the \mathbf{H}_{ext} applied along the a -axis at 293 K. The parameters used in the calculation are $H_E = 6.4 \times 10^6$ Oe, $H_D = 1.4 \times 10^5$ Oe, $\eta = 0.7$, $H_{ac} = 1.8 \times 10^3$ Oe, $H_{A2} = 3.3 \times 10^2$ Oe, and $H_E H_{ac} = 11\,600$ kOe², respectively.

(FWHM) of the corresponding absorption peaks. The spectral amplitude of AFM mode (circles) increases significantly as the magnetic field is larger than 4 T. It is consistent with the emergence of detectable AFM mode (Fig. 2(a)) and suggests an acceleration of SRT process in YFeO_3 with a relatively large applied magnetic field. As expected from the magnetic field induced SRT (inset of Fig. 3(a)), the transient torque \mathbf{T} is seen to decrease when the vector \mathbf{F} rotates from c -axis to a -axis. Thus, the spectral amplitude of FM mode is expected to be decreased with an increasing magnetic field along a -axis. However, one notices that the spectral amplitude of FM mode does not change a lot within our magnetic field range. In other words, our experimental results suggest that the component vector of \mathbf{F} along c -axis is kept constant. The explanation is, apart from the angle ϕ between the vector \mathbf{F} and a -axis becomes smaller during the SRT, the evolution of angle ϕ between vectors \mathbf{S}_1 and \mathbf{S}_2 cannot be ruled out, for the external magnetic field-induced SRT. Our measurements reveal a balance between these two contributions in YFeO_3 with an increasing magnetic field. In contrast, ϕ is in principle considered as constant within the SRT induced by temperature. Limited by our experimental condition, the maximum value of the magnetic field is up to 7 T along a -axis, the spins are mainly switched from Γ_4 to Γ_{24} . Even larger magnetic field of around 7.4 T was used to completely perform the SRT from Γ_4 to Γ_2 .³⁰

To better understand the SRT in YFeO_3 under external magnetic field in a quantitative picture, a simplified thermodynamic potential Φ , based on two-sublattice approximation is then expected as³¹

$$\Phi = A(\mathbf{S}_1 \mathbf{S}_2) + \frac{1}{2} a (S_{1z}^2 S_{2z}^2) + b S_{1z} S_{2z} - \mathbf{S}_1 \mathbf{H} + \mathbf{S}_2 \mathbf{H}, \quad (2)$$

where A is the exchange interaction parameter, a and b are the anisotropy parameters. In the case of a magnetic field

along the a -axis (i.e., $\theta=0$), the equilibrium values of the angle φ are given by^{32,33}

$$\left(\frac{\partial\Phi}{\partial\varphi}\right)_{M=M_0, \theta=0} = \cos\varphi(H_E H_{ac} \sin\varphi + H_E H_{A2} \sin^3\varphi - \eta H^2 \sin\varphi - HH_D) = 0, \quad (3)$$

where H_E is the effective symmetric exchange field, H_{ac} is the effective bilinear anisotropy fields in ac plane, H_{A2} is the effective biquadratic anisotropy fields in ac plane, H_D is the antisymmetric exchange field, and $\eta = (\chi_{\perp} - \chi_{\parallel})/\chi_{\perp}$, χ_{\perp} and χ_{\parallel} are the longitudinal and transverse antiferromagnetic susceptibilities, respectively. When $H \leq H_{cr}$, the sample system stays in the canted phase, the angle φ of the canted phase is governed by H ^{32,33}

$$H_E H_{A2} \sin^3\varphi + (H_E H_{ac} - \eta H^2) \sin\varphi - HH_D = 0. \quad (4)$$

The dynamical spin response can be solved by the Landau–Lifshitz–Gilbert (LLG) equation, detailed theory calculation can be found in supplementary material.²⁸ Figure 3(b) shows the results of calculated frequencies of FM (dashed line) and AFM mode (solid line) in the canted phase ($H \leq H_{cr}$), as a function of external magnetic field. The parameters we used here are $H_E = 6.4 \times 10^6$ Oe, $H_D = 1.4 \times 10^5$ Oe, $\eta = 0.7$, $H_{ac} = 1.8 \times 10^3$ Oe, $H_{A2} = 3.3 \times 10^2$ Oe, and $H_E H_{ac} = 11\,600$ kOe².³³ When we increase the external magnetic field, the frequency of FM mode decreases, which is well consistent with the data of Fig. 2. The frequency of AFM increases first, and then decreases within the whole magnetic field range. In this work, a resonant frequency at about 0.54 THz is observed with high magnetic fields above 4 T. Given that the AFM mode (0.527 THz) has been reported with zero external magnetic field at room temperature,¹⁵ we therefore expect the frequency of AFM mode has a slight increased tendency as the magnetic field is increased to 4 T, which coincides with our calculation results. Our experimental results emphasize that the observable SRT occurs as the external magnetic field is larger than 4 T.

The similar experiments have been also performed on a NdFeO₃ single crystal. However, one can observe different spin switching. For example, cooling of NdFeO₃ from 170 to 100 K leads to a continuous rotation of \mathbf{F} from c - to a -axis and an irreversible switching between Γ_4 and Γ_2 is attributed to the anisotropy of Nd³⁺. Our findings here indicate that Y or rare-earth ions play an important role in the SRT of orthoferrite antiferromagnetic single crystal.

In summary, the THz-TDS has been used for investigation of the dynamical SRT in YFeO₃ single crystal. Owing to be absence of $4f$ -electrons in Y ion, the spin reorientation of Fe sublattices can only be induced by the applied magnetic field, rather than temperature. Our data are in agreement with a simplified thermodynamic model with two-sublattice approximation. Furthermore, compared with the magnetic field-induced SRT of NdFeO₃, we clearly demonstrate the difference of spin switching of Fe ions. Given that the anisotropy can be significantly modified by rare-earth ions, we foresee lots of opportunities to design spin switching in the orthoferrite systems.

The research was supported by National Natural Science Foundation of China (Nos. 11174195, 50932003, 11274221), Ph.D. Programs Foundation of Ministry of Education of China (No. 20123108110003), and the Research Innovation Fund of the Shanghai Education Committee (No. 14ZZ101).

¹G. Cinader, *Phys. Rev.* **155**, 453 (1967).

²M. D. Lumsden, B. C. Sales, D. Mandrus, S. E. Nagler, and J. R. Thompson, *Phys. Rev. Lett.* **86**, 159 (2001).

³M. R. Moldover, G. Sjolander, and W. Weyhmann, *Phys. Rev. Lett.* **26**, 1257 (1971).

⁴J. Scola, Y. Dumont, N. Keller, M. Vallée, J. G. Caputo, I. Sheikin, P. Lejay, and A. Pautrat, *Phys. Rev. B* **84**, 104429 (2011).

⁵Y. Cao, S. Cao, W. Ren, Z. Feng, S. Yuan, B. Kang, B. Lu, and J. Zhang, *Appl. Phys. Lett.* **104**, 232405 (2014).

⁶W. C. Koehler, E. O. Wollan, and M. K. Wilkinson, *Phys. Rev.* **118**, 58 (1960).

⁷H. Shen, Z. Cheng, F. Hong, J. Xu, S. Yuan, S. Cao, and X. Wang, *Appl. Phys. Lett.* **103**, 192404 (2013).

⁸S. N. Barilo, *Sov. Phys. Solid State* **33**, 354 (1991).

⁹L. T. Tsymbal, Y. B. Bazaliy, V. N. Derkachenko, V. I. Kamenev, G. N. Kakazei, F. J. Palomares, and P. E. Wigen, *J. Appl. Phys.* **101**, 123919 (2007).

¹⁰S. R. Brown and I. Hall, *J. Phys.: Condens. Matter* **5**, 4207 (1993).

¹¹A. V. Kimel, A. Kirilyuk, P. A. Usachev, R. V. Pisarev, A. M. Balbashov, and Th. Rasing, *Nature* **435**, 655 (2005).

¹²A. Kirilyuk, A. V. Kimel, and Th. Rasing, *Rev. Mod. Phys.* **82**, 2731 (2010).

¹³A. V. Kimel, B. A. Ivanov, R. V. Pisarev, P. A. Usachev, A. Kirilyuk, and Th. Rasing, *Nat. Phys.* **5**, 727 (2009).

¹⁴T. Kampfrath, A. Sell, G. Klatt, A. Pashkin, S. Mahrlein, T. Dekorsy, M. Wolf, M. Fiebig, A. Leitenstorfer, and R. Huber, *Nat. Photonics* **5**, 31 (2011).

¹⁵K. Yamaguchi, M. Nakajima, and T. Suemoto, *Phys. Rev. Lett.* **105**, 237201 (2010).

¹⁶Z. Jin, Z. Mics, G. Ma, Z. Cheng, M. Bonn, and D. Turchinovich, *Phys. Rev. B* **87**, 094422 (2013).

¹⁷K. Yamaguchi, T. Kurihara, Y. Minami, M. Nakajima, and T. Suemoto, *Phys. Rev. Lett.* **110**, 137204 (2013).

¹⁸J. Jiang, Z. M. Jin, G. B. Song, X. Lin, G. H. Ma, and S. X. Cao, *Appl. Phys. Lett.* **103**, 062403 (2013).

¹⁹A. V. Kimel, A. Kirilyuk, and Th. Rasing, *Laser Photon. Rev.* **1**, 275 (2007).

²⁰Z. M. Jin, H. Ma, L. H. Wang, G. H. Ma, F. Y. Guo, and J. Z. Chen, *Appl. Phys. Lett.* **96**, 201108 (2010).

²¹I. Dzyaloshinsky, *J. Phys. Chem. Solids* **4**, 241 (1958).

²²T. Moriya, *Phys. Rev.* **120**, 91 (1960).

²³H. Lutgemeir, H. G. Bohn, and M. Brajczewska, *J. Magn. Magn. Mater.* **21**, 289 (1980).

²⁴Y. B. Bazaliy, L. T. Tsymbal, G. N. Kakazei, A. I. Izotov, and P. E. Wigen, *Phys. Rev. B* **69**, 104429 (2004).

²⁵W. Slawinski, R. Przenioslo, I. Sosnowska, and E. Suard, *J. Phys.: Condens. Matter* **17**, 4605 (2005).

²⁶G. W. Durbin, C. E. Johnson, and M. F. Thomas, *J. Phys. C: Solid State Phys.* **8**, 3051 (1975).

²⁷R. Z. Zhou, Z. M. Jin, G. F. Li, G. H. Ma, Z. X. Cheng, and X. L. Wang, *Appl. Phys. Lett.* **100**, 061102 (2012).

²⁸See supplementary material at <http://dx.doi.org/10.1063/1.4913998> for typical time domain spectroscopy, its Fourier transform spectroscopy and calculation of the resonant frequencies.

²⁹A. A. Volkov, Yu. G. Goncharov, G. V. Kozlov, K. N. Kocharyan, S. P. Lebedev, A. S. Prokhorov, and A. M. Prokhorov, *Pis'ma Zh. Eksp. Teor. Fiz.* **39**, 140 (1984) [*JETP Lett.* **39**, 166 (1984)].

³⁰J. Scola, W. Noun, E. Popova, A. Fouchet, Y. Dumont, and N. Keller, *Phys. Rev. B* **81**, 174409 (2010).

³¹Y. A. Izyumov and V. N. Syromyatnikov, *Phase Transition and Crystal Symmetry* (Springer, Berlin, 1990).

³²I. S. Jacobs, H. F. Burne, and L. M. Levinson, *J. Appl. Phys.* **42**, 1631 (1971).

³³A. M. Balbashov, A. G. Berezin, Yu. M. Gufan, G. S. Kolyadko, P. Yu. Marchukov, and E. G. Rudashevsky, *Sov. Phys. JETP* **66**, 174 (1987).